JOURNAL OF COMPUTATIONAL PHYSICS 107, 201–212 (1993)

Spectral Approximation to Advection–Diffusion Problems by the Fictitious Interface Method

A. FRATI AND F. PASQUARELLI

Dipartimento di Matematica, Università Cattolica, Brescia, Italy

AND

A. QUARTERONI

Dipartimento di Matematica, Politecnico di Milano, Milano, Italy and
School of Mathematics and Minnesota Supercomputer Institute, University of Minnesota, Minneapolis, Minnesota

Received October 23, 1990; revised August 30, 1991

In this work we face the numerical approximation by spectral methods of advection-diffusion equations for convective dominated regimes. For either boundary and internal layer problems, it has been recently pointed out that effective methods can be based on dropping the viscous terms far from the thin layer. This yields a problem that couples two different model equations (one of hyperbolic type, the other one of parabolic type) through suitable matching conditions at subdomain interfaces. An extensive theory has been developed and effective algorithms have been derived. Here we apply this theory to spectral approximations to two-dimensional steady problems. In particular, we investigate the issues of stability and convergence, and we propose effective algebraic solvers to face both the hyperbolic and elliptic problems.

INTRODUCTION

In this paper we analyse numerical approximation to advection–diffusion problems in which the effects of the diffusion term are prominent only on a small region of the computational domain. Problems of this type can be found, for example, in the study of the motion of viscous and compressible fluids around rigid profiles and in problems of thermal diffusion.

This solution behaviour allows the identification on the computational domain of two portions in which the problem is well represented either by the full advection–diffusion equation or by a reduced advection equation that can be obtained by dropping the viscous terms. The main problem arising from this coupled model is to fix the correct conditions at the fictitious interface Γ separating the two regions in order to allow for a correct transmission of information between the different types of equations.

This problem has been studied in [5], where it has been shown that the flux continuity should be enforced across the whole Γ, whereas the continuity of the physical solution needs to be satisfied only on that portion of the interface where the flow leaves the "viscous" domain and enters the "inviscid" one.

It is, furthermore, possible to solve the coupled problem by an iterative scheme that allows for an independent solution of the two subproblems. In this way one can even use two different numerical solvers, according to the different nature of each problem.

In this paper we apply the spectral collocation method to the solution of the coupled problem in a two-dimensional domain. In particular, we first investigate the spectral solution of the two subproblems (the reduced advection equation and the complete advection–diffusion equation). We enforce the (inflow) boundary conditions implicitly, and we solve the related systems by the GMRES method by the help of suitable finite difference preconditioners. These two independent solvers are then used within the framework of the iterative procedures that is proposed for the coupled viscous–inviscid problem.

We analyze the effect of the interface location on the jump between the two solutions, as well as the behaviour of the rate of convergence of the subdomain iterations in terms of the critical parameters such as the viscosity, the convective velocity and the number of collocation points that are being used. Several examples of advection–diffusion problems whose solution exhibits a boundary layer are approximated. Considerations on the relation between stability and the Peclet number are given. We conclude with an application of our method to a nonlinear time-dependent advection–diffusion problem.

0021-9991/93 $5.00

1. THE ADVECTION PROBLEM

In this section we investigate a spectral collocation method to approximate a hyperbolic equation in a two-dimensional domain $\Omega = (-1, 1)^2$. Let b_0 and $\mathbf{b}$ be a scalar and a two-dimensional vector-valued function defined in Ω, respectively. We consider the following problem:

$$\text{find } u: \Omega \to \mathbb{R} \text{ such that}$$

$$\operatorname{div}(\mathbf{b}u) + b_0 u = f \qquad \text{in } \Omega \tag{1.1}$$

$$u = \lambda \qquad \text{on } \partial\Omega^{\text{in}}, \tag{1.2}$$

where, if $\mathbf{n}$ denotes the unit normal vector to $\partial\Omega$ oriented outward, $\partial\Omega^{\text{in}} = \{x \in \partial\Omega \mid \mathbf{b} \cdot \mathbf{n} < 0\}$ is the region of $\partial\Omega$, where the flux is going into Ω (see Fig. 1.1 for two examples). The two functions $\lambda: \partial\Omega^{\text{in}} \to \mathbb{R}$ and $f: \Omega \to \mathbb{R}$ are given from data. We set, moreover, $\partial\Omega^{\text{out}} = \partial\Omega \backslash \partial\Omega^{\text{in}}$; $\partial\Omega^{\text{in}}$ and $\partial\Omega^{\text{out}}$ are termed inflow and outflow boundaries, respectively.

Let $\mathbb{P}_N$ denote the space of algebraic polynomials of degree $\leqslant N$ with respect to each variable x and y. We consider the following one-dimensional Gauss–Lobatto–Legendre quadrature formula (see, e.g., [2]):

$$\sum_{j=0}^{N} u(\eta_j)\, \theta_j \cong \int_{-1}^{1} u\, dx, \tag{1.3}$$

where $\eta_0 = 1$, $\eta_N = -1$, and η_j, for $1 \leqslant j \leqslant N-1$, are the zeros of the derivative of the Legendre polynomial P_N of degree N (see, e.g., [11]). The coefficients θ_j are given by

$$\theta_j = \begin{cases} \dfrac{2}{N(N+1)}, & j = 0 \text{ and } j = N \\ \dfrac{-2}{N+1} \left(P_N(\eta_j)\, P'_{N-1}(\eta_j)\right)^{-1}, & 1 \leqslant j \leqslant N-1. \end{cases} \tag{1.4}$$

Equality occurs in (1.3) whenever u is a polynomial of degree less than or equal to $2N-1$. We denote now by $\Xi_N = \{(x_i, y_j),\ 0 \leqslant i, j \leqslant N\}$ the set of $(N+1)^2$ points obtained with the cartesian product of the knots η_j, and by Ξ_N^0 the subset of those $(N-1)^2$ points of Ξ_N internal to Ω.

For any vector function $\mathbf{v} = (v_1, v_2)^{\mathrm{T}}$ defined on $\bar{\Omega}$, we denote by $I_N \mathbf{v}$ the vector $(\tilde{v}_1, \tilde{v}_2)^{\mathrm{T}}$, where $\tilde{v}_k \in \mathbb{P}_N$ is the interpolating polynomial of v_k at the points of Ξ_N $(k = 1, 2)$. Finally, if Σ is a subset of $\partial\Omega$, we set $\Sigma_N = \Sigma \cap \Xi_N$.

We can now introduce the following numerical approximation to the problem (1.1)–(1.2),

$$\text{find } u_N \in \mathbb{P}_N \text{ such that}$$

$$L_N u_N + b_0 u_N = f \qquad \text{at } \Xi_N^0 \cup \partial\Omega_N^{\text{out}} \tag{1.5}$$

$$u_N = \lambda \qquad \text{at } \partial\Omega_N^{\text{in}}, \tag{1.6}$$

where

$$L_N v := \tfrac{1}{2} \{\operatorname{div}(I_N(\mathbf{b}v)) + \mathbf{b} \cdot \nabla v + v \operatorname{div}(I_N \mathbf{b})\}$$

is a skew-symmetric approximation of $\operatorname{div}(\mathbf{b}v)$. Precisely, one has

$$(L_N v, w)_{N,\Omega} = -(L_N w, v)_{N,\Omega} \qquad \forall v, w \in \mathbb{P}_N,$$

where

$$(u, v)_{N,\Omega} = \sum_{(x_i, y_j) \in \Xi_N} u(x_i, y_j)\, v(x_i, y_j)\, \theta_i \theta_j \tag{1.7}$$

is a two-dimensional discrete inner product generated by the quadrature formula (1.3).

Figure 1.2 shows in a schematical way the different role of the collocation points for the case considered in Fig. 1.1a.

We consider now instead of (1.5)–(1.6) the problem,

$$\text{find } u_N \in \mathbb{P}_N \text{ such that}$$

$$L_N u_N + b_0 u_N = f \qquad \text{at } (\Xi_N^0 \cup \partial\Omega_N^{\text{out}}) \tag{1.8}$$

$$\mathbf{b} \cdot \mathbf{n}(u_N - \lambda)(x_i, y_j) = (L_N u_N + b_0 u_N - f)(x_i, y_j)\, \theta_{k(i,j)} \quad \forall (x_i, y_j) \in \partial\Omega_N^{\text{in}}, \tag{1.9}$$

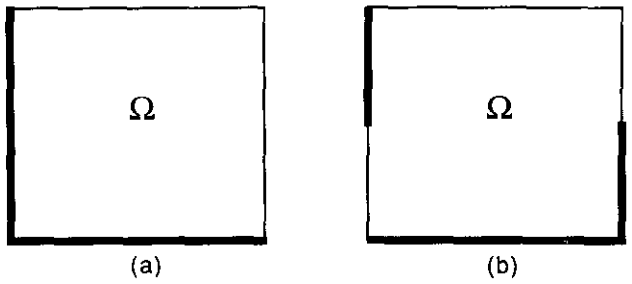

FIG. 1.1. Inflow and outflow boundary for the two cases: $\mathbf{b} = (1, 1)^{\mathrm{T}}$ (case (a)) and $\mathbf{b} = (y, 1)^{\mathrm{T}}$ (case (b)). The solid lines of $\partial\Omega$ denote the inflow boundary $\partial\Omega^{\text{in}}$.

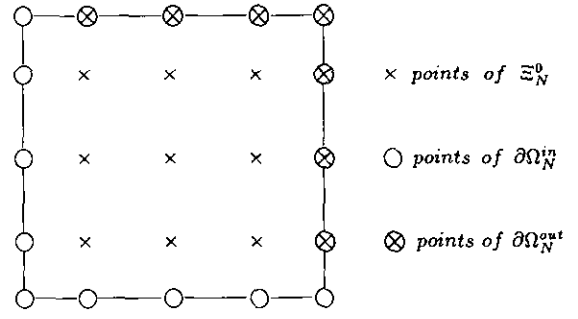

FIG. 1.2. The subset Ξ_N^0, $\partial\Omega_N^{\text{in}}$ and $\partial\Omega_N^{\text{out}}$ for the test case of Fig. 1.1a.

where $k(i, j) = j$ (resp., i) if (x_i, y_j) belongs to a horizontal side (resp., vertical side) of $\partial\Omega$.

The coefficient $\theta_{k(i,j)}$ that multiplies the value of the residual of the equation in (1.9) is proportional to N^{-2}; hence as N tends to infinity, the right-hand side of (1.9) tends to zero yielding in the limit the inflow boundary condition satisfied exactly at $\partial\Omega_N^{\text{in}}$, as it was in (1.6).

Remark 1.1. The corner points of Ω deserve special attention. Figure 1.3 reports the three cases of flux on the corners that may occur: a corner point Q is of *outflow* type if it separates two sides belonging to $\partial\Omega_N^{\text{out}}$ (case α); it is of *inflow* type if both sides sharing Q belong to $\partial\Omega_N^{\text{in}}$ (case β), it is of *inflow/outflow* type if one side belongs to $\partial\Omega_N^{\text{in}}$, whereas the other belongs to $\partial\Omega_N^{\text{out}}$ (case γ). The equation written for each case is described below:

$$(\alpha) \qquad (L_N u_N + b_0 u_N)(x_0, y_0) = f(x_0, y_0)$$

$$(\beta) \qquad (\theta_N \mathbf{b}\cdot\mathbf{n}_1 + \theta_0 \mathbf{b}\cdot\mathbf{n}_2)(u_N - \lambda)(x_0, y_0) = (L_N u_N + b_0 u_N - f)(x_0, y_0)\,\theta_N\theta_0$$

$$(\gamma) \qquad \theta_0 \mathbf{b}\cdot\mathbf{n}_2 (u_N - \lambda)(x_0, y_0) = (L_N u_N + b_0 u_N - f)(x_0, y_0)\,\theta_N\theta_0.$$

Each equation has been obtained by taking as test function v in the formula (1.10) below the Lagrange polynomial relative to the corner Q, i.e., the polynomial $v \in \mathbb{P}_N : v(Q) = 1$, $v(T) = 0$ for all $T \in \Xi_N$, $T \neq Q$.

Concerning accuracy, the problem (1.8)–(1.9) enjoys the same properties of problem (1.5)–(1.6). However, it is more suitable than (1.5)–(1.6) to be analyzed. As a matter of fact, (1.8)–(1.9) turns out to be equivalent to the following problem, which is the variational discrete formulation to the problem (1.1)–(1.2) (see, e.g., [5]):

$$(L_N u_N, v)_{N,\Omega} + (b_0 u_N, v)_{N,\Omega} - (\mathbf{b}\cdot\mathbf{n} u_N, v)_{N,\partial\Omega^{\text{in}}} = (f, v)_{N,\Omega} - (\mathbf{b}\cdot\mathbf{n}\lambda, v)_{N,\partial\Omega^{\text{in}}} \qquad \forall v \in \mathbb{P}_N. \quad (1.10)$$

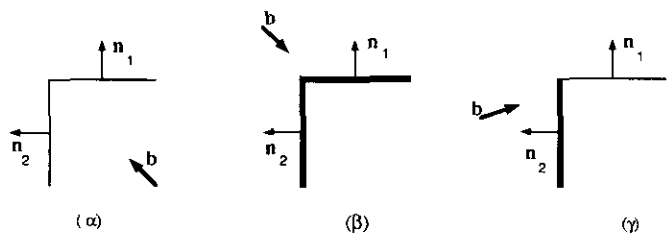

FIG. 1.3. Corner points of outflow, inflow, and inflow/outflow type, respectively.

In [5] it is proven that if there exists $\beta_N > 0$ such that

$$\tfrac{1}{2}\,\text{div}[I_N \mathbf{b}(p)] + b_0(p) \geqslant \beta_N > 0 \qquad \forall p \in \Omega,$$

then (1.10) is stable in the sense that

$$\beta_N \|u_N\|^2_{N,\Omega} + |u_N|^2_{N,\partial\Omega^{\text{out}}} \leqslant \frac{1}{\beta_N}\|f\|^2_{N,\Omega} + |\lambda|^2_{N,\partial\Omega^{\text{in}}}, \quad (1.11)$$

where $\|\cdot\|_{N,\Omega}$ is the norm associated to (1.7), $|v|_{N,\Sigma} = (|\mathbf{b}\cdot\mathbf{n}|, v^2)^{1/2}_{N,\Sigma}$, where for all $\Sigma \subset \partial\Omega$, $(\cdot,\cdot)_{N,\Sigma}$ is the one-dimensional scalar product generated by (1.3) and restricted to the nodes of Σ. The formulation (1.10) allows one to enforce in a natural way the inflow boundary conditions at all points of $\partial\Omega_N^{\text{in}}$. In particular, one can deduce from (1.10) the proper way to satisfy the inflow condition at those nodes of $\partial\Omega_N^{\text{in}}$ that are either corner points of Ω, or points separating the inflow from the outflow boundary. This has been pointed out in the Remark 1.1.

Remark 1.2. The inflow boundary treatment that we have adopted is a generalization of a similar one formerly proposed by Funaro and Gottlieb [3] for Chebyshev approximations to one-dimensional problems. Indeed, both approaches lead to a penalty technique to enforce the boundary conditions. Here we have derived such a treatment as a result of the variational discrete formulation (1.10) of the spectral collocation problem. Our interpretation allows in particular the derivation of the correct boundary treatment of corner points. We can obtain an approximation scheme like (1.5)–(1.6) using the Gauss–Lobatto–Chebyshev points as well. However, in this case since the Chebyshev weight function is singular on the boundary, the weak formulation (1.10) no longer holds. Numerical results of the following subsection show that, in order to obtain a stable Chebyshev approximation, the coefficient $\theta_{k(i,j)}$ in (1.10) (that in the Chebyshev case is proportional to N^{-1}) needs to be replaced with a constant proportional to N^{-2}. This conclusion is in agreement with the one obtained in [3] for the one-dimensional case.

1.1. *Numerical Solution to the Advection Problem* (1.8)–(1.9)

This subsection deals with the algorithmic aspects of the scheme (1.8)–(1.9). We report in addition the numerical results obtained for some test problems. Let

$$\mathbf{Lu} = \mathbf{F} \quad (1.12)$$

be the linear system associated with (1.8)–(1.9). The vector $\mathbf{u}$ contains the $(N+1)^2$ unknown values of u_N at the collocation points of Ξ_N. The system has been solved using the GMRES (generalized minimal residual) algorithm. Briefly, this algorithm can be described as follows (see, e.g., [9]):

TABLE I

The Number of GMRES Iterations for the Case (a) with Several Preconditioners and Several Values of N

N	7	9	11	13	15	17	19
Not prec.	38	59	79	105	139	167	$\geqslant 500$
$\mathbf{L}_{FD}$	5	7	10	18	24	35	80
$\tilde{\mathbf{L}}^1_{FD}$	4	6	8	10	11	13	14
$\tilde{\mathbf{L}}^2_{FD}$	4	4	5	6	7	8	10

Let $\mathbf{x}_0$ be an initial guess; we consider the Krylov space K_M generated by $\{\mathbf{r}_0, \mathbf{L}\mathbf{r}_0, ..., \mathbf{L}^{M-1}\mathbf{r}_0\}$, where $\mathbf{r}_0 = \mathbf{F} - \mathbf{L}\mathbf{x}_0$ is the residue associated with $\mathbf{x}_0$. We then compute $\bar{\mathbf{x}}$ so that the new residue $\bar{\mathbf{r}} = \mathbf{F} - \mathbf{L}\bar{\mathbf{x}}$ is minimum on K_M. In particular, if M is equal to the dimension of $\mathbf{L}$, $\bar{\mathbf{x}}$ is the exact solution of the system. Since the method is generally used with a smaller M (in order to reduce its computational complexity), the computed vector $\bar{\mathbf{x}}$ is set equal to $\mathbf{x}^1$ and the iterations go on until a desired accuracy is obtained.

We stress now that the matrix $\mathbf{L}$ of the system (1.12) is ill conditioned (its condition number grows like a constant time N^2). Thus the number of iterations that are needed to converge is big, even taking M sufficiently large. This implies that both the computational cost and the memory space necessary to implement the method are large when the dimension of the problem increases, and, by consequence, the iterative method is not competitive with a direct resolution. In order to lower the condition number we solve by the GMRES method the following preconditioned system:

$$\mathbf{L}_{FD}^{-1}\mathbf{L}\mathbf{u} = \mathbf{L}_{FD}^{-1}\mathbf{F} \tag{1.13}$$

In a first attempt, the preconditioning matrix $\mathbf{L}_{FD}$ can be obtained by approximating the problem (1.1) by a centered finite difference scheme at the same grid points of Ξ_N. An even better preconditioner $\tilde{\mathbf{L}}_{FD}$ can be obtained by approximating, still by a centered finite difference scheme, the following problem instead of (1.1)

$$-\varepsilon_n \Delta u + \operatorname{div}(\mathbf{b}u) + b_0 u = f \qquad \text{in } \Omega \tag{1.14}$$

TABLE II

The Number of GMRES Iterations for the Case (b) with Several Preconditioners and Several Values of N

N	7	9	11	13	15	17	19
Not prec.	56	121	213	360	$\geqslant 500$	$\geqslant 500$	$\geqslant 500$
$\mathbf{L}_{FD}$	4	5	8	11	17	24	29
$\tilde{\mathbf{L}}^1_{FD}$	4	5	6	8	10	13	16
$\tilde{\mathbf{L}}^2_{FD}$	4	5	6	8	10	12	13

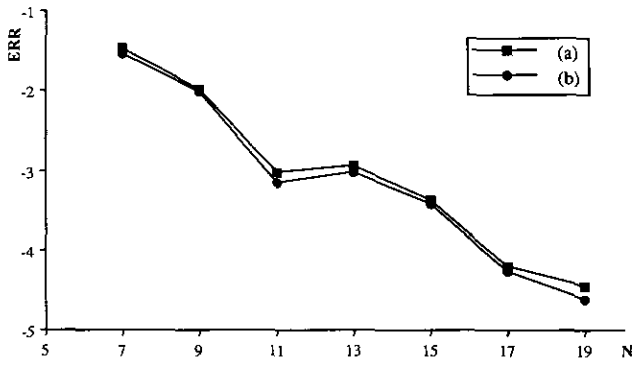

FIG. 1.4. The logarithm of the maximum norm of the error for the cases of Tables I and II.

where ε_n is a properly chosen numerical viscosity. The Tables I and II report the iteration numbers obtained using the GMRES without preconditioners and with three different preconditioners. In particular, we note by $\tilde{\mathbf{L}}^1_{FD}$ the matrix associated to $\varepsilon_n = C_1$ and by $\tilde{\mathbf{L}}^2_{FD}$ the matrix related to $\varepsilon_n = C_2 \sin(\pi(x+1)/2) \sin(\pi(y+1)/2)$, where C_1 and C_2

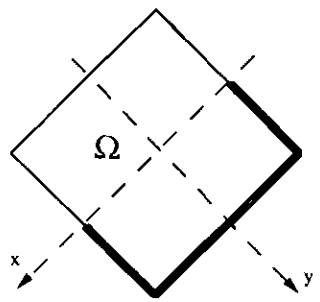

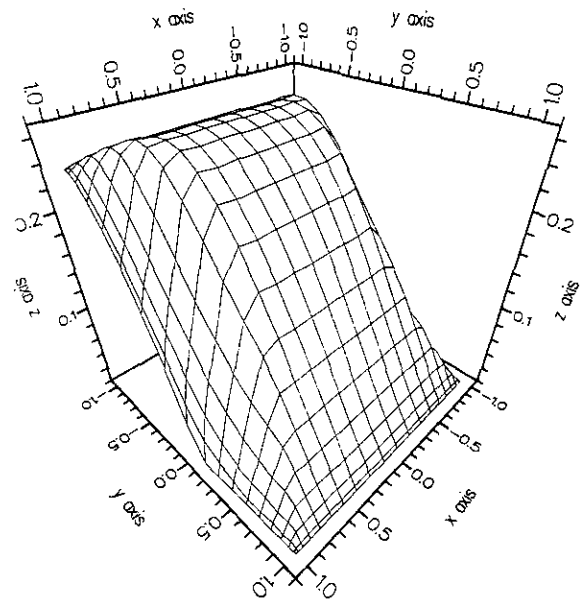

FIG. 1.5. The computed solution for $\mathbf{b} = 5(-xy, -1)^T$.

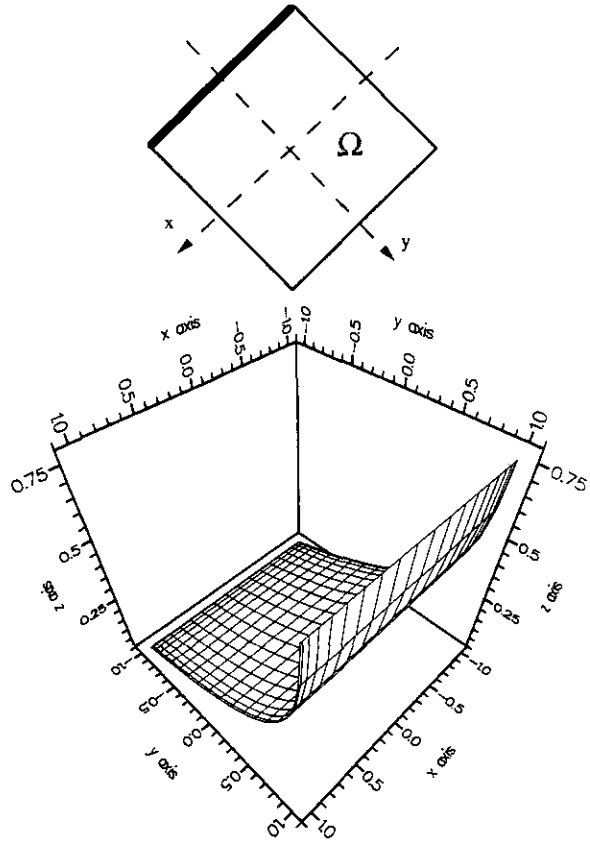

FIG. 1.6. The computed solution for $\mathbf{b} = 5(x, (1-y))^T$.

are constants. These results are referred to the cases (a) and (b) of Fig. 1.1, for an exact solution $u(x, y) = \sin(\pi y)\,\mathrm{arctg}(4(1+x))$. The iterative method is stopped when the residual is less than 10^{-8}. M is fixed to 10, C_1 and C_2 are equal to 0.03 and 0.1, respectively, for the case (a) and to 0.005 and 0.03 for the case (b).

Figure 1.4 reports the relative errors $(u - u_N)$, in the maximum norm, between the exact solution and the spectral solution, for several values of N, for both cases (a) and (b) shown in Fig. 1.1. We report now in Figs. 1.5, 1.6 some results obtained with the scheme (1.8)–(1.9). In the margin of every picture we draw the domain Ω in which the shaded boundary denotes the inflow boundary. The solution corresponds to taking $f = 1$ as the right-hand side and $u = 0$ at all inflow boundary points.

In the following example, we show that the solution obtained by the collocation Chebyshev scheme (1.8)–(1.9) presents uncontrolled oscillations (see Fig. 1.7). These oscillations do not decrease when the number of collocation points is increased. The solution of the Legendre scheme for the same problem is instead sufficiently accurate (see Fig. 1.8). To obtain an accurate solution by a Chebyshev scheme, we must replace the coefficient $\theta_{k(i,j)}$ in (1.9) with the value $(2N^2-1)/(2N^2-N)(N^2-1)$ as indicated in [3]. The solution obtained using the new scheme is practically indistinguishable from the one obtained by the Legendre method.

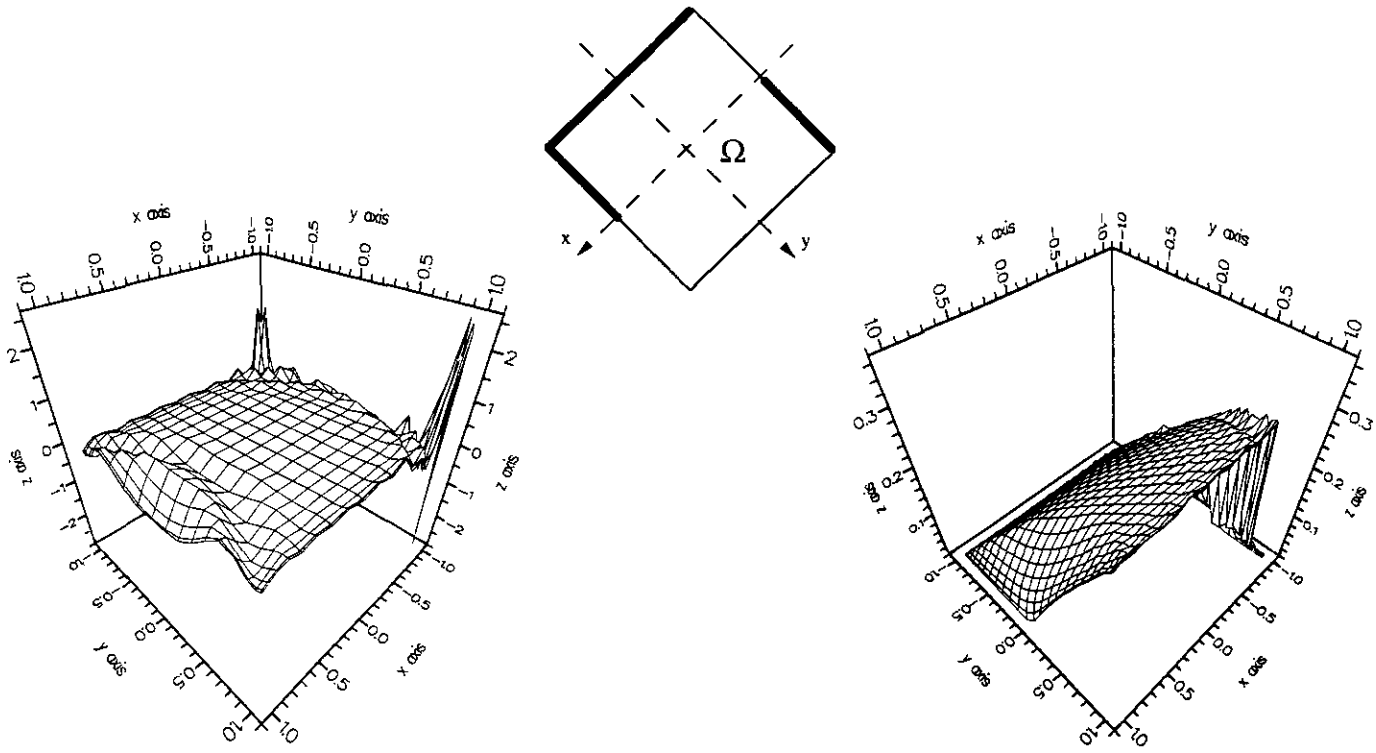

FIG. 1.7. The computed solution with the Chebyshev scheme for $\mathbf{b} = 5(y, 1)^T$.

FIG. 1.8. The computed solution with the Legendre scheme for $\mathbf{b} = 5(y, 1)^T$.

2. THE ADVECTION–DIFFUSION PROBLEM

In this section we analyze a collocation approximation scheme for the advection–diffusion equation

$$-\varepsilon \Delta u + \operatorname{div}(\mathbf{b}u) + b_0 u = f \qquad \text{in } \Omega. \tag{2.1}$$

To assign the boundary conditions, let Γ^D and Γ^{Ne} be two subsets of Ω such that $\Gamma^D \cap \Gamma^{Ne} = \varnothing$ and $\Gamma^D \cup \Gamma^{Ne} = \partial\Omega$. We assume that

$$\frac{\partial u}{\partial \mathbf{n}} = g \qquad \text{on } \Gamma^{Ne} \tag{2.2}$$

$$u = h \qquad \text{on } \Gamma^D, \tag{2.3}$$

where g and h are two given functions.

Since we are interested in approximating problems where the viscosity ε is small, we are sure that $\mathbf{b} \cdot \mathbf{n} \geqslant 0$ on Γ^{Ne}. This prevents incompatibility conditions when the flow is dominated by the convection. Using the same notations of the previous section, we obtain now the following collocation scheme:

$$\text{find } u_N \in \mathbb{P}_N \text{ such that}$$

$$-\varepsilon \Delta u_N + L_N u_N + b_0 u_N = f \qquad \text{at } \Xi_N^0 \tag{2.4}$$

$$-\varepsilon \left(\frac{\partial u_N}{\partial \mathbf{n}} - g \right)(x_i, y_j) = (-\varepsilon \Delta u_N + L_N u_N + b_0 u_N - f)(x_i, y_j)\, \theta_{k(i,j)} \qquad \forall (x_i, y_j) \in \Gamma_N^{Ne} \tag{2.5}$$

$$u_N(x_i, y_j) = h(x_i, y_j) \qquad \forall (x_i, y_j) \in \Gamma_N^D. \tag{2.6}$$

(The index $k(i, j)$ in (2.5) is the same as used in (1.9).)

The Neumann condition (2.2) has been enforced variationalwise at the outflow collocation points of Γ_N^{Ne}. A stability analysis of (2.4)–(2.6) is carried out in [5].

Numerical results are obtained solving the linear system associated with the scheme (2.4)–(2.6) by a preconditioned GMRES method. The preconditioning matrix is now obtained via an incomplete factorization of the matrix of finite differences for the problem (2.1)–(2.3). This technique, which is known as row sum agreement incomplete factorization, is described, e.g., in [1, Chap. 5]. The two following tables report the GMRES iteration numbers for several values of ε. The dimension of the Krylov subspace is $M = 10$. For both cases the exact solution of the advection problem (2.1) is $u(x, y) = \sin(\pi y) \operatorname{arctg}(4(1 + x))$. The coefficients are $b_0 = 0$ and $\mathbf{b} = (1, 1)^T$ for Table III, whereas $\mathbf{b} = (y, 1)^T$ for Table IV. The right-hand side f is obtained accordingly. About the boundary conditions, Neumann data are enforced on the upper side of Ω, whereas Dirichlet data are enforced on the three remaining sides.

TABLE III

The Number of GMRES Iterations for the Problem (2.4)–(2.6) with $\mathbf{b} = (1, 1)^T$

N	7	9	11	13	15	17	19
$\varepsilon = 0.1$	2	2	2	2	2	2	2
$\varepsilon = 0.01$	5	7	8	9	10	10	11
$\varepsilon = 0.001$	5	9	12	19	27	40	51

TABLE IV

The Number of GMRES Iterations for the Problem (2.4)–(2.6) with $\mathbf{b} = (y, 1)^T$

N	7	9	11	13	15	17	19
$\varepsilon = 0.1$	2	2	2	2	2	2	2
$\varepsilon = 0.01$	4	4	5	5	6	6	6
$\varepsilon = 0.001$	4	6	8	11	15	20	24

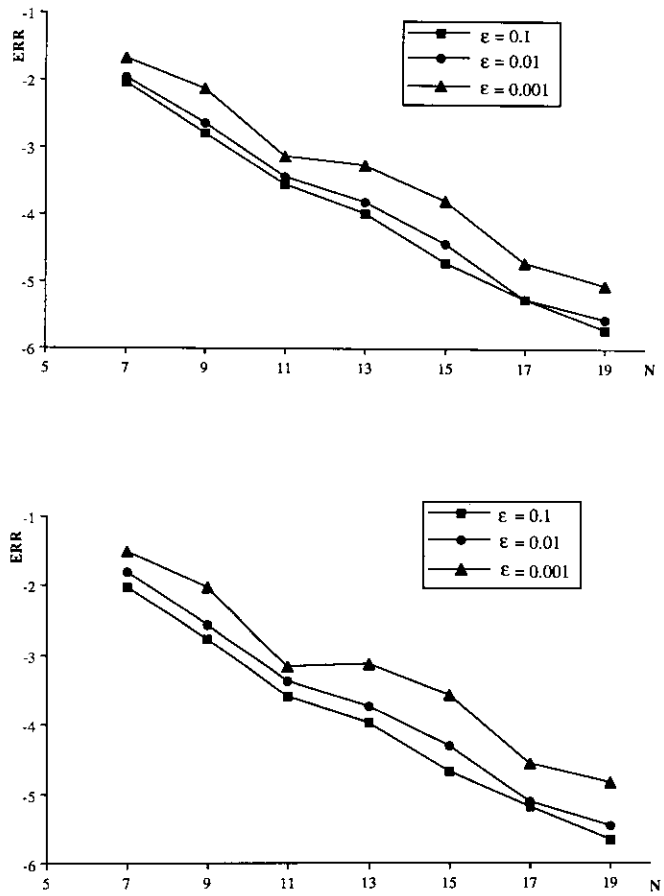

FIG. 2.1. The logarithm of the maximum norm of the error for the cases of Tables III and IV.

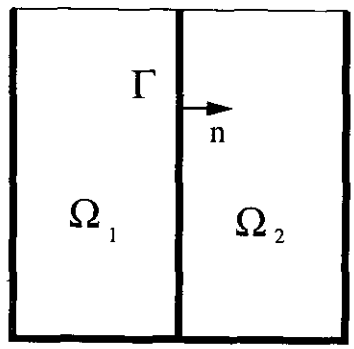

FIG. 2.2. The decomposition of Ω into two subdomains.

We show in Fig. 2.1 the maximum norm of the relative error $(u-u_N)$ for several values of N and ε. It is clear that a way to improve the effectiveness of the above collocation method is to resort to a domain decomposition technique. For instance, one can subdivide Ω into two disjoint subdomains, Ω_1 and Ω_2 as indicated in Fig. 2.2, then look for two polynomial solutions u_N^1, u_N^2 that satisfy a collocation problem in Ω_1 and Ω_2, respectively, and the prescribed boundary conditions on $\partial\Omega_1 \cap \partial\Omega$ and $\partial\Omega_2 \cap \partial\Omega$. Moreover, u_N^1 and u_N^2 should be continuous on $\Gamma = \partial\Omega_1 \cap \partial\Omega_2$, and their fluxes should match, i.e.,

$$\varepsilon \frac{\partial u_N^1}{\partial \mathbf{n}} - \mathbf{b}\cdot\mathbf{n} u_N^1 = \varepsilon \frac{\partial u_N^2}{\partial \mathbf{n}} - \mathbf{b}\cdot\mathbf{n} u_N^2$$

at all collocation points lying on Γ. Here $\mathbf{n}$ is the normal outward vector to Ω_1 as indicated in Fig. 2.2.

It is well known that a domain decomposition approach yields generally a better accuracy, and higher geometrical flexibility than the single domain one. An inside advantage is the fact that domain decomposition approximations generally allow a weaker restriction on N to obtain stability. As a matter of fact, it is known that, in order to prevent oscillations issuing from critical layers, one should use a polynomial degree sufficiently large with respect to the Peclet number, which in turns is proportional to $|\mathbf{b}|\,\varepsilon^{-1}$.

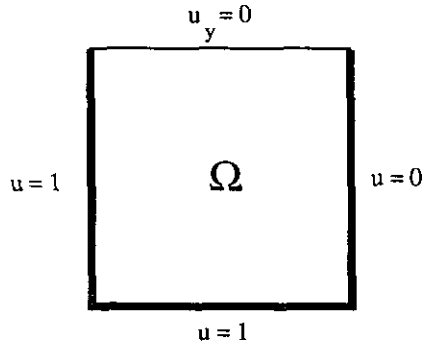

FIG. 2.3. The boundary conditions for the problem (2.7).

TABLE V

The Lowest Value of the Number of Degrees of Freedom Ensuring a Collocation Solution Free of Oscillations for the Problem (2.7), for Both the Single-Domain and the Multidomain Approach (with Two Subdomains)

	Single-domain		Two-domain	
ε	$\beta=1$	$\beta=5$	$\beta=1$	$\beta=5$
0.1	100	400	66	190
0.05	196	748	66	276
0.01	784	>1600	190	496
0.005	1600	>1600	276	780

A convenient position of the interface Γ allows one to obtain a multidomain solution free of oscillations with a number of collocation points significantly smaller than the one needed for the standard single-domain spectral solution. As an example, let us consider the problem

$$-\varepsilon \Delta u + \beta\left(\frac{\partial u}{\partial x} + \frac{\partial u}{\partial y}\right) = 0 \qquad \text{in } (-1,1)^2 \qquad (2.7)$$

with the boundary conditions indicated in Fig. 2.3. For several values of ε and β, Table V reports the lowest number of degrees of freedom for which the spectral solution is free of oscillations. We remind that the number of degrees of freedom pertaining to a spectral solution of degree N is $(N+1)^2$ in the single-domain case and $(2N+1)(N+1)$ in the two-domain case. For the problem at hand, the interface is the vertical line $x = 1-\sqrt{\varepsilon}$.

3. THE COUPLING OF HYPERBOLIC AND ELLIPTIC EQUATIONS VIA THE FICTITIOUS INTERFACE METHOD

In this section we consider a (steady) advection–diffusion equation in Ω for which the viscosity effects are dimensionally negligible apart from a small subregion Ω_2 of Ω. This consideration suggests to solve the complete equation only on Ω_2 and to solve in the complementary region $\Omega_1 = \Omega\backslash\Omega_2$ a reduced advection equation obtained dropping the diffusion term. In this way, one is left with a hyperbolic problem in Ω_1 and an elliptic problem in Ω_2. Across the interface $\Gamma = \partial\Omega_1 \cap \partial\Omega_2$, we must impose correct transmission conditions that ensure the consistency between the original problem and the coupled one. Such conditions, that have been investigated in [5], state that continuity of the flux must hold across the whole Γ, whereas the continuity of the solution needs to be satisfied only on the subset Γ^{in} of Γ, where the flow goes from the elliptic domain Ω_2 to the "hyperbolic" domain Ω_1. We consider therefore instead of

(2.1) the following problem: *find a pair of functions u, v defined respectively in Ω_1 and Ω_2 such that:*

$$\operatorname{div}(\mathbf{b}u) + b_0 u = f \qquad \text{in } \Omega_1 \qquad (3.1)$$

$$-\varepsilon \Delta v + \operatorname{div}(\mathbf{b}v) + b_0 v = f \qquad \text{in } \Omega_2 \qquad (3.2)$$

$$u = \phi \qquad \text{on } \Gamma_1^{\text{in}} \qquad (3.3)$$

$$v = \phi \qquad \text{on } \Gamma_2^{D} \qquad (3.4)$$

$$\frac{\partial v}{\partial \mathbf{n}_2} = g \qquad \text{on } \Gamma_2^{Ne} \qquad (3.5)$$

$$-\varepsilon \frac{\partial v}{\partial \mathbf{n}_2} + \mathbf{b} \cdot \mathbf{n}_2 v = -\mathbf{b} \cdot \mathbf{n}_1 u \qquad \text{on } \Gamma \qquad (3.6)$$

$$u = v \qquad \text{on } \Gamma^{\text{in}}. \qquad (3.7)$$

The subsets Γ_1^{in} and Γ_1^{out} are, respectively, the inflow and outflow boundary of the subdomain Ω_1, whereas Γ_2^D and Γ_2^{Ne} are the portions of $\partial\Omega_2$ where, respectively, Dirichlet and Neumann boundary conditions are enforced. $\mathbf{n}_k$ denotes the outward unit normal vector on $\partial\Omega_k$, for $k = 1, 2$. The problem (3.1)–(3.7) can now be approximated on each side by the collocation schemes proposed in the previous sections.

We report now some pictures that represent the computed spectral solution of some test problems. Aside from any graphics, we draw the partition of Ω; the solid boundary denotes either the inflow boundary for Ω_1 or the Dirichlet boundary for Ω_2. In Fig. 3.1 we report the solution of the problem obtained by choosing $\varepsilon = 0.01$, $\mathbf{b} = ((y - 2x), 1)^T$, $b_0 = 0$, and $f = 1$, and homogeneous boundary conditions. In all our numerical tests, the polynomial degree of the spectral solution within each subdomain is $N = 20$ (this amounts to 441 gridpoints).

We consider now the problem (2.1) with $\mathbf{b} = (0, 1)^T$, i.e.,

$$-\varepsilon \Delta w + w_y = 0 \qquad (3.8)$$

with boundary conditions indicated in Fig. 2.3. The solution of this problem has a boundary layer of thickness

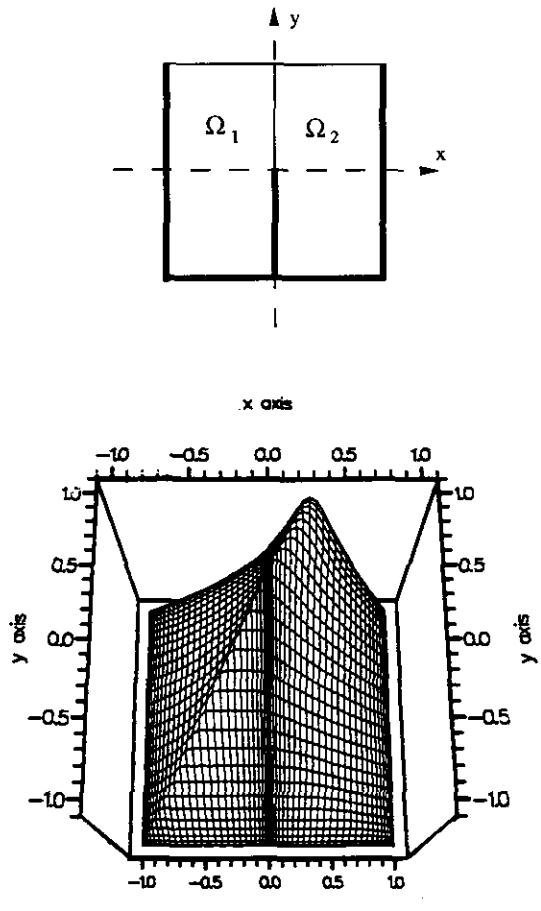

FIG. 3.1. The solution of the coupled problem for the case $\mathbf{b} = ((y - 2x), 1)^T$.

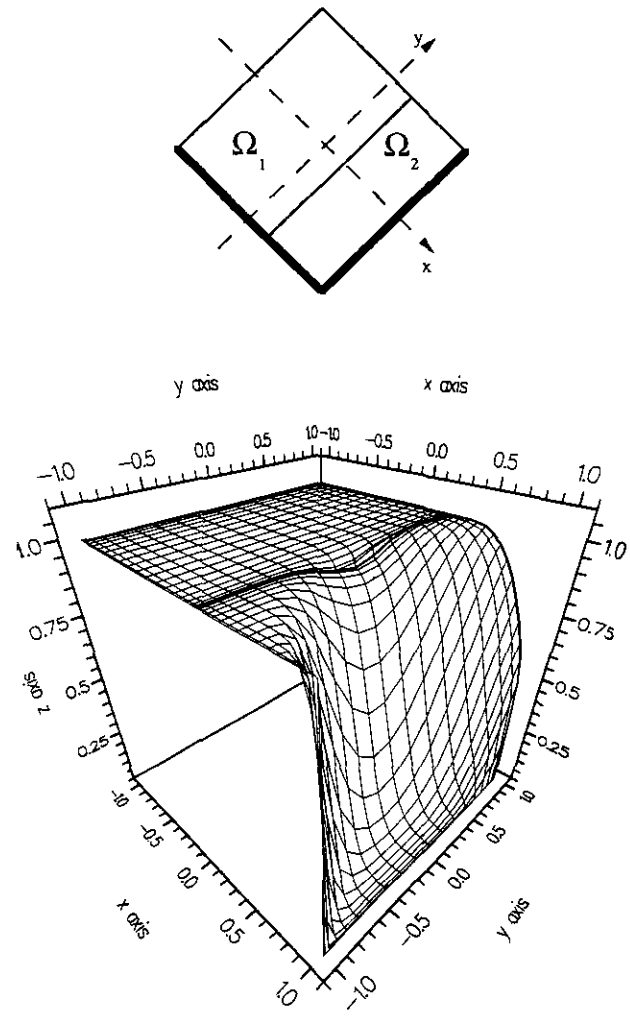

FIG. 3.2. The solution of (3.8) for $\varepsilon = 0.001$.

$O(\sqrt{\varepsilon})$ near the right side of Ω. We consider a decomposition of Ω for which $\Gamma = \{(x, y) \mid x = 1 - 8\sqrt{\varepsilon}\}$. Figures 3.2 and 3.3 show the numerical solutions relative to $\varepsilon = 0.001$ and $\varepsilon = 0.0001$. In both cases they are very accurate.

In [5] it has been shown that the solution of the problem (3.1)–(3.7) can be computed as a limit of solutions of two subproblems within Ω_1 and Ω_2, respectively. Precisely, let us note first that the conditions (3.6), (3.7) can be replaced by the following equivalent conditions:

$$-\varepsilon \frac{\partial v}{\partial \mathbf{n}_2} + \mathbf{b} \cdot \mathbf{n}_2 v = -\mathbf{b} \cdot \mathbf{n}_1 u \qquad \text{on } \Gamma^{\text{out}} \tag{3.9}$$

$$-\varepsilon \frac{\partial v}{\partial \mathbf{n}_2} = 0 \qquad \text{on } \Gamma^{\text{in}} \tag{3.10}$$

$$u = v \qquad \text{on } \Gamma^{\text{in}} \tag{3.11}$$

One can then solve the hyperbolic problem in Ω_1 with the boundary conditions (3.11) on Γ^{in}, and the elliptic problem

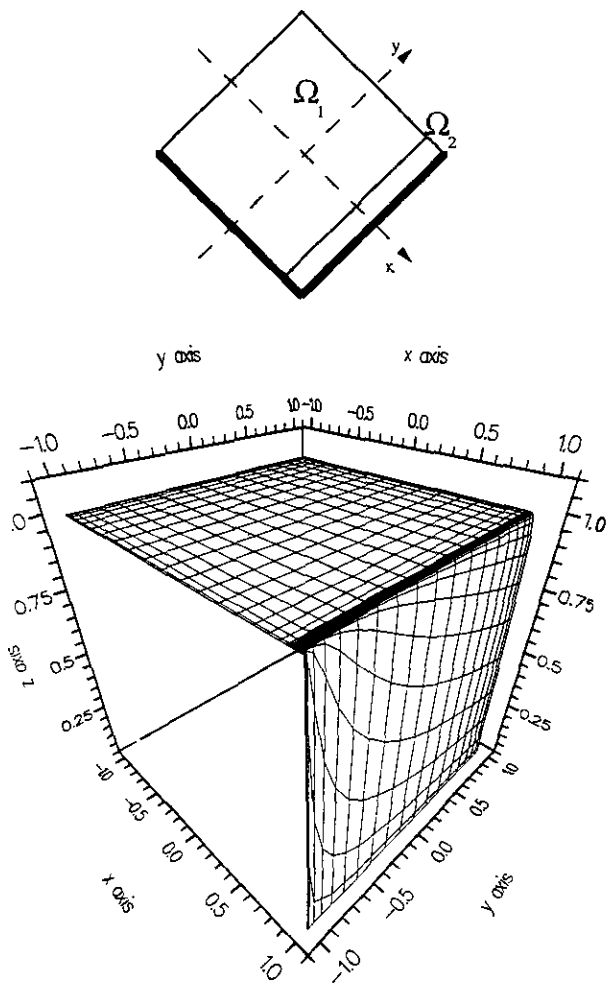

FIG. 3.3. The solution of (3.8) for $\varepsilon = 0.0001$.

in Ω_2 with the boundary conditions (3.9), (3.10) on the interface Γ. The numerical collocation approximation of these problems can then be obtained using the following iterative procedure:

Let u^0, v^0 be given on Γ^{in}; for each n, we look for two polynomials $u_N^n \in \mathbb{P}_N$, $v_N^n \in \mathbb{P}_N$ such that

$$\begin{aligned}
&L_{N,1} u_N^n + b_0 u_N^n = f \qquad \text{at } \Xi_{N,1}^0 \cup \Gamma_{N,1}^{\text{out}} \cup \Gamma_N^{\text{out}} \\
&\mathbf{b} \cdot \mathbf{n}_1 (u_N^n - \phi) = (L_{N,1} u_N^n + b_0 u_N^n - f)\, \theta_{1,k(i,j)} \qquad \text{at } \Gamma_{N,1}^{\text{in}} \\
&\mathbf{b} \cdot \mathbf{n}_1 (u_N^n - \psi^n) = (L_{N,1} u_N^n + b_0 u_N^n - f)\, \theta_{1,k(i,j)} \qquad \text{at } \Gamma_N^{\text{in}}
\end{aligned} \tag{3.12}$$

and

$$\begin{aligned}
&-\varepsilon\, \Delta v_N^n + L_{N,2} v_N^n + b_0 v_N^n = f \qquad \text{at } \Xi_{N,2}^0 \\
&v_N^n = \phi \qquad \text{at } \Gamma_{N,2}^D \\
&-\varepsilon \left(\frac{\partial v_N^n}{\partial \mathbf{n}_2} - g \right) = (-\varepsilon\, \Delta v_N^n + L_{N,2} v_N^n \\
&\qquad + b_0 v_N^n - f)\, \theta_{2,k(i,j)} \qquad \text{at } \Gamma_{N,2}^{Ne} \\
&-\varepsilon \frac{\partial v_N^n}{\partial \mathbf{n}_2} + \mathbf{b} \cdot \mathbf{n}_2 (v_N^n - u_N^n) = (-\varepsilon\, \Delta v_N^n + L_{N,2} v_N^n \\
&\qquad + b_0 v_N^n - f)\, \theta_{2,k(i,j)} \qquad \text{at } \Gamma_N^{\text{out}} \\
&-\varepsilon \frac{\partial v_N^n}{\partial \mathbf{n}_2} = (-\varepsilon\, \Delta v_N^n + L_{N,2} v_N^n \\
&\qquad + b_0 v_N^n - f)\, \theta_{2,k(i,j)} \qquad \text{at } \Gamma_N^{\text{in}},
\end{aligned} \tag{3.13}$$

where, for $n \geqslant 1$, $\psi^n = \rho v_N^{n-1} + (1 - \rho)\, u_N^{n-1}$; ρ is a positive acceleration parameter that is dynamically computed in order to minimize at each step the error on the interface Γ_N^{in}. The coefficients $\theta_{1,k(i,j)}$ in Ω_1 and $\theta_{2,k(i,j)}$ in Ω_2 are defined as in the previous sections.

There are two cases in which one of the two problems (3.12), (3.13) is independent of the other. Precisely, (3.13) is independent of (3.12) if $\Gamma_N^{\text{out}} = \varnothing$, whereas (3.12) is independent of (3.13) if $\Gamma_N^{\text{in}} = \varnothing$. In these situations the iterative procedure converges, of course, in one iteration.

Let NIT be the minimum value of n such that

$$\max_{p \in \Gamma_N} \frac{|u_N^n(p) - u_N^{n-1}(p)|}{|u_N^n(p)|} \leqslant 10^{-8}.$$

We show in Figs. 3.4 and 3.5 some results relative to the case $\mathbf{b} = \beta(y(x+1), 1)^{\mathrm{T}}$ that summarize the behaviour of NIT for various choices of ε, N, and $\mathbf{b}$. They show that NIT is independent of the number of grid points, whereas it has a very mild dependence on the size of ε and $|\mathbf{b}|$. These results

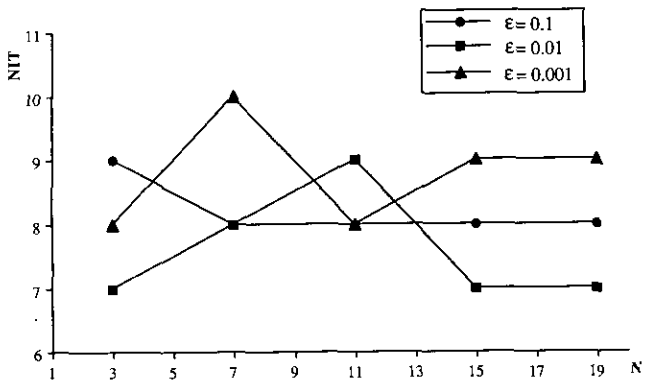

FIG. 3.4. The iteration number for different values of N (β is equal to 1).

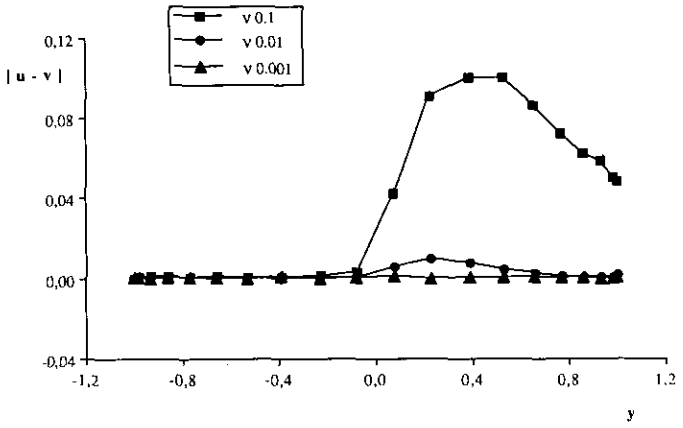

FIG. 3.6. The jump on Γ for $\mathbf{b} = ((y-2x), 1)$.

are in agreement with the theoretical conclusions obtained in [5].

We rewind that the global solution $w_N = \{u_N \text{ in } \Omega_1; v_N \text{ in } \Omega_2\}$ of the coupled problem (3.12)–(3.13) is continuous only on the subset Γ^{in} of Γ. For smooth problems, the value of the jump across Γ^{out} ($=\Gamma \backslash \Gamma^{in}$) is proportional to ε (see, e.g. [7]). In Fig. 3.6, we report the jump on Γ for the test problem of Fig. 3.1, for several values of ε. On the other hand, if the solution exhibits a boundary layer, the interface Γ should be located outside the boundary layer (but not too far from it) (see [6]). In Fig. 3.7, we report the maximum value of the jump, for several values of ε. We take $\Gamma = \{(\bar{x}, y), -1 < y < 1\}$ for three different values of $\bar{x}$. The considered problem is obtained with $\mathbf{b} = (1, 1)^T$, $b_0 = 1$, and $f = 1$ and the boundary conditions are indicated in Fig. 2.3. The solution of this problem exhibits a boundary layer of thickness $O(\varepsilon)$ near the vertical wall of Ω. We note, however, that also in this case, the jump is of order ε whenever the interface Γ is properly chosen. Note that for $\bar{x} = 1 - \varepsilon$ the interface is within the boundary layer region.

We emphasize now some potential advantages of the proposed approach. Since the subproblems defined in Ω_1 and Ω_2 need to be solved separately, one can in principle use a different solver for the hyperbolic problem than for the elliptic one. Moreover, as for the multidomain elliptic–elliptic approach described at the conclusion of Section 2, the restriction on N in terms of the Peclet number is weaker than in the case of a single-domain approach.

We also remind that the number of iteration of the multidomain elliptic–elliptic scheme increases when ε decreases. Such a resolution technique is therefore expensive for convection dominated equations. On the contrary, we have shown that the iteration number of the scheme (3.12)–(3.13) for the coupled hyperbolic–elliptic problem is practically independent of ε.

Remark 3.1. (Time dependent problems). We consider now the problem

$$\frac{\partial u}{\partial t} - \varepsilon \Delta u + \operatorname{div}(\mathbf{b}u) + b_0 u = f. \tag{3.14}$$

Discretizing (3.14) in time by an implicit finite difference scheme, we must solve at any temporal level an advection–diffusion problem like (2.1). We can then use the iterative scheme (3.12)–(3.13) to compute the solution at the new

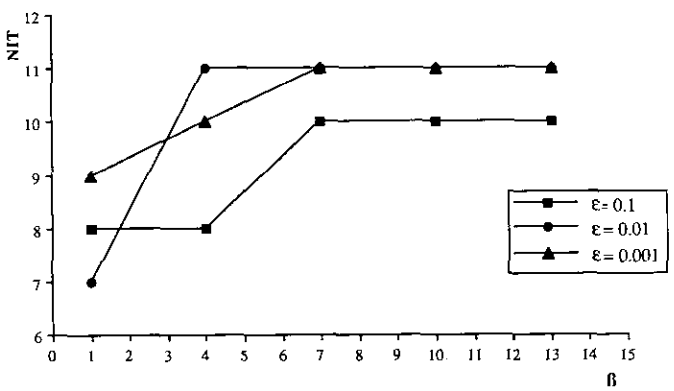

FIG. 3.5. The iteration number for different values of β (N is equal to 15).

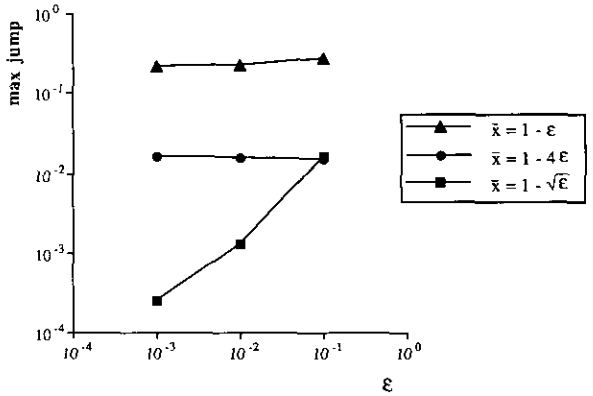

FIG. 3.7. The maximum jump for several values of ε and for several position of Γ for $\mathbf{b} = (1, 1)^T$.

time. For an explicit time-advancing scheme, the interface conditions need to be enforced at the new time-level, yielding a two by two system to be solved at each gridpoint on Γ.

4. EXTENSION TO THE NONLINEAR CASE

In this last section we are interested in extension of the previous approach to a time dependent nonlinear advection–diffusion equation. We consider, for instance, the model problem,

$$\frac{\partial w}{\partial t} - \varepsilon \Delta w + \mathbf{b}(w) \cdot \nabla w + b_0 w = f \qquad \text{in} \quad \Omega \times (0, T), \quad (4.1)$$

where $\mathbf{b}(w)$ is a vector function depending on w. We introduce first a temporal approximation. We note by w^k the value of w at the time $(k\,\Delta t)$, where Δt is the temporal discretization parameter. Equation (4.1) can now be discretizated in time, for instance, by a scheme dealing with all terms implicitly except for $\mathbf{b}(w)$ which is taken at the previous time level. The simplest scheme of this family reads

$$-\varepsilon \Delta w^{k+1} + \mathbf{b}(w^k) \cdot \nabla w^{k+1} + \left(\frac{1}{\Delta t} + b_0\right) w^{k+1} = \frac{w^k}{\Delta t} + f^{k+1}, \qquad k = 0, 1, 2, \ldots. \quad (4.2)$$

In this way at each time-level we need to solve an advection–diffusion problem like the one faced in the previous section. Interface conditions between the hyperbolic subdomain Ω_1 and the elliptic subdomain Ω_2 become

$$\begin{aligned} -\mathbf{b}(u^k) \cdot \mathbf{n}_1 u^{k+1} &= \varepsilon \frac{\partial v^{k+1}}{\partial \mathbf{n}_1} - \mathbf{b}(v^k) \cdot \mathbf{n}_1 v^{k+1} \qquad \text{on } \Gamma \\ u^{k+1} &= v^{k+1}, \qquad \text{where} \quad \mathbf{b}(u^k) \cdot \mathbf{n}_1 < 0, \end{aligned} \quad (4.3)$$

where u^{k+1} and v^{k+1} denote the solution in Ω_1 and Ω_2, respectively.

Then we can use the scheme (3.12)–(3.13) to approximate (4.2)–(4.3). We consider now a test problem investigated in [10] in which $\Omega = (-1, 1)^2$, $b_0 = f = 0$, $\mathbf{b}(w) = (w, \sigma)^T$, where σ is a constant and the initial condition is

$$w_0(x, y) = \tfrac{1}{2}(1 + y - xy - 5x).$$

Although initially smooth, the solution of this problem develops an internal layer at some finite time of width $O(\varepsilon)$. This fact suggests that we use a decomposition of Ω into three subdomains instead of two. In this way we can solve the complete equation only in the central domain $\Omega_2 =$ $(0, 0.4) \times (-1, 1)$, where the solution exhibits a sharp layer. In the remaining subdomains $\Omega_1 = (-1, 0) \times (-1, 1)$ and $\Omega_3 = (0.4, 1) \times (-1, 1)$ we solve the reduced advection equation solely. The iteration procedure for this case can be easily obtained by adapting the one described in the previous section.

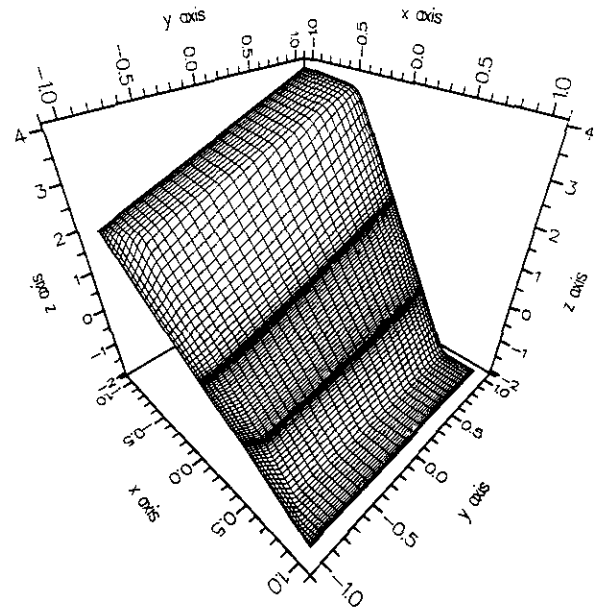

FIG. 4.1. The solution of the nonlinear problem (4.1) at the time $t = 0.15$.

As boundary conditions, we prescribe $w(x, y, t) = w_0(x, y)\ \forall t > 0$ for all points (x, y) belonging to the lower horizontal as well as the two vertical sides of Ω. Further, we

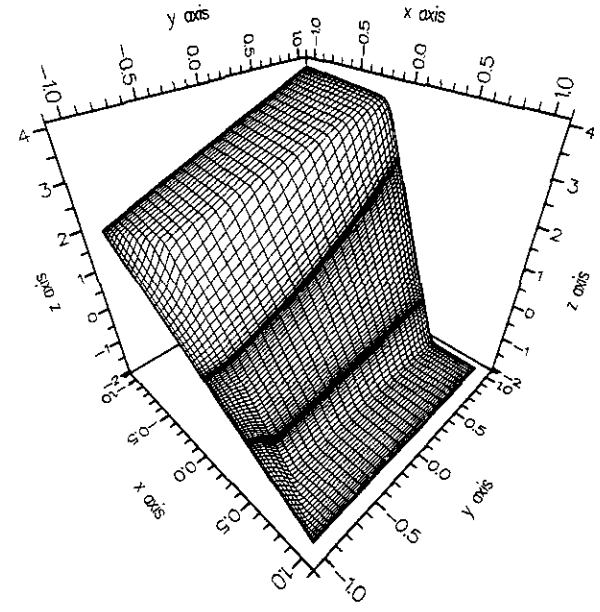

FIG. 4.2. The solution of the nonlinear problem (4.1) at the time $t = 0.20$.

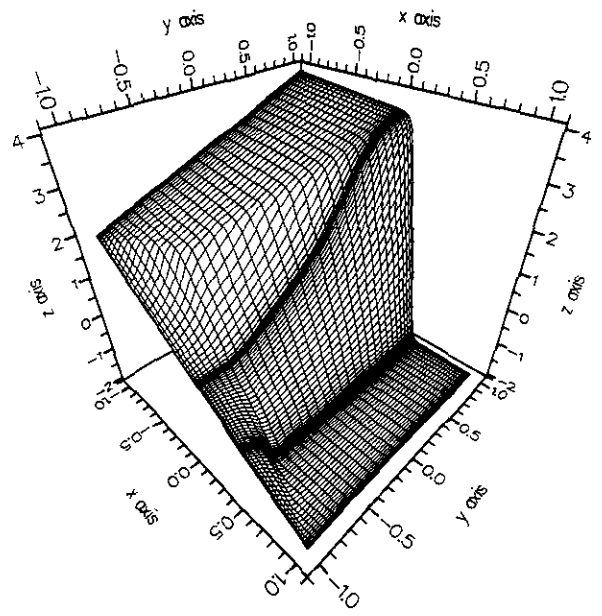

FIG. 4.3. The solution of the nonlinear problem (4.1) at the time $t = 0.30$.

satisfy a homogeneous Neumann condition on the upper horizontal side of Ω_2.

We report some pictures that represent the computed solution for different time levels. This solution refers to the values $\varepsilon = 0.1 \times 10^{-4}$, $\sigma = 1$; we have taken $\Delta t = 0.12 \times 10^{-3}$ and $(34)^2$ collocation points in each subdomain. We plot the solution at the time levels $t = 0.15$ (Fig. 4.1), $t = 0.20$ (Fig. 4.2), and $t = 0.30$ (Fig. 4.3). We can see that the coupling relationships (4.3) yield a very accurate numerical solution of the nonlinear problem at hand.

5. CONCLUSION AND DISCUSSION

We have discussed the algorithmic aspects of the so-called fictitious interface method for the numerical approximation of convection-dominated flows. This method is based on the assumption that the viscous terms can be dropped outside tiny regions embodying the critical layers.

The solution algorithm relies on alternating the solution of advection equation and the one of advection–diffusion equation within complementary subdomains. To this end, we have presented efficient algebraic solvers (based upon the preconditioned GMRES method) to face either advection or advection–diffusion boundary-value problems.

For all problems here considered, the spatial discretization is achieved by the spectral collocation method using Legendre–Gaussian nodes. Several numerical tests have been carried out on linear problems; further, an application of the fictitious interface method to a nonlinear Burgers equation is shown. A systematic approach to nonlinear problems is presented in [6]. In all example here considered, the interface location was decided a priori (according to the physical nature of the expected solution). In more general situations (e.g., in time-dependent and/or non-linear problems), the location of the interface would be better chosen dynamically, or else by a control procedure. Also this issue is discussed in [6].

REFERENCES

1. C. Canuto, M. Y. Hussaini, A. Quarteroni, and T. A. Zang, *Spectral Methods in Fluid Dynamics* (Springer-Verlag, New York/Heidelberg/Berlin, 1988).
2. P. J. Davis and P. Rabinowitz, *Methods of Numerical Integration*, 2nd ed. (Academic Press, London/New York, 1984).
3. D. Funaro and D. Gottlieb, *Math. Comput.* **51**, 599 (1988).
4. F. Gastaldi and A. Quarteroni, On the Coupling of Hyperbolic and Parabolic Systems: Analytical and Numerical Approach, *Appl. Numer. Math.* **6**, 3 (1989).
5. F. Gastaldi, A. Quarteroni, and G. Sacchi Landriani, in *Domain Decomposition Methods for Partial Differential Equations, III*, edited by T. F. Chan *et al.* (SIAM, Philadelphia, 1990), p. 22.
6. A. Quarteroni, F. Pasquarelli, and A. Valli, in *Domain Decomposition Methods for Partial Differential Equations, V*, edited by D. E. Keyes *et al.* (SIAM, Philadelphia, 1992), p. 129.
7. A. Quarteroni and A. Valli, in *Domain Decomposition Methods for Partial Differential Equations, IV*, edited by R. Glowinski *et al.* (SIAM, Philadelphia, 1991), p. 58.
8. G. Rodrigue and E. Reiter, in *Domain Decomposition Methods for Partial Differential Equations, II*, edited by T. F. Chan *et al.* (SIAM, Philadelphia, 1990), p. 226.
9. Y. Saad and M. H. Schultz, *SIAM J. Sci. Stat. Comput.* **7**, 856 (1986).
10. J. S. Scroggs, in *Domain Decomposition Methods for Partial Differential Equations, III*, edited by T. F. Chan *et al.* (SIAM, Philadelphia, 1990), p. 373.
11. G. Szego, *Orthogonal Polynomials* (Amer. Math. Soc., New York, 1939).